Hindawi
Science and Technology of Nuclear Installations
Volume 2019, Article ID 1041486, 9 pages
https://doi.org/10.1155/2019/1041486

Research Article

A Modified Multiobjective Self-Adaptive Differential Evolution Algorithm and Its Application on Optimization Design of the Nuclear Power System

Yunjia Yang,[1,2] Shinian Peng,[1,2] Li Zhu,[2] Dan Zhang,[1,2] Zhifang Qiu,[1,2] Hongsheng Yuan,[1,2] and Lin Xian[1,2]

[1]*Science and Technology on Reactor System Design Technology Laboratory, Chengdu 610041, China*
[2]*Nuclear Power Institute of China, Chengdu 610041, China*

Correspondence should be addressed to Shinian Peng; 1695083738@qq.com

Received 1 April 2019; Revised 3 May 2019; Accepted 16 May 2019; Published 4 August 2019

Academic Editor: Arkady Serikov

A modified multiobjective self-adaptive differential evolution algorithm (MMOSADE) is presented in this paper to improve the accuracy of multiobjective optimization design in the nuclear power system. The performance of the MMOSADE is tested by the ZDT test function set and compared with classical evolutionary algorithms. The results indicate that MMOSADE has a better performance in convergence and diversity. Based on the MMOSADE, a multiobjective optimization design platform for the nuclear power system is proposed, and the application of which is carried out. The evaluation program of the PRHR-HX in AP1000 is developed, and its reliability is verified. The optimal design schemes of PHHR-HX are obtained by utilizing the multiobjective optimization design platform. The results show that the optimal design schemes can envelop the prototype design scheme. This conclusion proves that the optimization design platform proposed in this paper is effective and feasible.

1. Introduction

Taking the nuclear safety system as an example, the current design method of nuclear power system mainly adopts the linear iteration mode of trial-evaluation-correction. This method not only consumes a lot of workforce, computational resources, and time, but also has difficulty in obtaining an overall optimal design scheme on safety and economy. In recent years, with the development of the computer technology and optimization algorithm, researchers have carried out the application research of multiobjective optimization in the field of nuclear power system design. At present, the multiobjective optimization design of nuclear power plants is mainly based on predefining weighting factors for different optimal targets to translate the multiobjective optimization problems (MOP) into single-objective optimization problems [1–3]. This method relies heavily on the engineer's design experience because of the need to assign weights to different targets. However, there are certain mutual constraints and conflicts among the optimization targets for the optimization design of nuclear power system. The weighting method is complicated to solve this kind of problems effectively. In response to the above issues, Chen et al. [4–6] carried out a series of studies on MOP of nuclear power systems based on the nondominated sorting genetic algorithm-II (NSGA-II). This algorithm applies the concept of "Pareto optimal solution" [7], which can directly deals with MOP and obtain all relatively optimal solutions that satisfy the design requirements.

The main purpose of the multiobjective optimization design for nuclear power system is replacing a large amount of repetitive work performed by engineers in the design process, obtaining qualified reference schemes, and providing more scientific and integrated data support for the final technical decision-making. Therefore, for the multiobjective optimization design of nuclear power system, a superior multiobjective optimization algorithm should have the advantage that the calculated solution can cover the real solutions of the MOP as much as possible. That is, it has a higher requirement on the convergence and diversity of the algorithm. The

differential evolution algorithm (DE) is a random heuristic search algorithm proposed by Storn and Price [8]. It is simple and easy to utilize. Moreover, DE has strong robustness and global optimization ability [9]. According to what has been discussed above, DE is more suitable for nuclear power system which has the characteristics of numerous parameters, strong coupling, and nonlinear response.

To further improve the convergence and diversity of multiobjective optimal design results of nuclear power system, a modified multiobjective differential evolution algorithm (MMOSADE) is developed. Based on MMOSADE, a nuclear power system multiobjective optimization design platform is developed. The feasibility and reliability of the platform are verified by the AP1000 nuclear power plant passive residual heat removal heat exchanger (PRHR-HX).

The organization of this paper is as follows. This section presents the background and motivation of the research. In the second section, the multiobjective optimization problem and Pareto optimal solution are introduced briefly, and MMOSADE is described in detail. The multiobjective optimization platform for nuclear power system is presented and applied in the third section. In the last section, the research conclusions are summarized and the prospects are put forward.

2. Modified Multiobjective Differential Evolution Algorithm

In this section, the concept of multiobjective optimization problem and Pareto optimal solution are explained. Based on standard DE, the MMOSADE is developed by introducing strategies of other evolutionary algorithms and improved method of the NSGA-II crowding-distance calculation.

2.1. MOP and Pareto Optimal Solution. In the field of nuclear power system optimal design, MOPs often need to be processed by the concept of Pareto optimal solution. Take the safety system as an example, it requires higher safety and better economy. However, improving the safety of nuclear power plants usually means more economic cost. The main purpose of the multiobjective optimization algorithm based on Pareto optimal solution is to solve the MOPs with conflicting and restrictive effects among different targets.

Taking minimization problem as an example, a MOP can be expressed by (1).

$$\begin{aligned} \min_{X\in R} \quad & F(X) = \left[f_1(X), f_2(X), \ldots, f_n(X)\right] \\ s.t. \quad & g_i(X) \le 0 \\ & h_j(X) = 0 \\ & R = \left\{X \mid g_i(X) \le 0,\ h_j(X) = 0\right\} \\ & X = \left[x_1, x_2, \ldots, x_k\right] \end{aligned} \tag{1}$$

where $F(X)$ is a set of objective functions; $f_1(X), f_2(X), \ldots, f_n(X)$ are subobjective functions; X is a k-dimension optimization variable; R is a feasible region; $g_i(X)$ and $h_j(X)$ are inequality constraints and equality constraints, respectively.

Assuming that vector X and vector U are feasible solutions for the MOP. If the condition shown by (2) is satisfied, it can be considered that U dominates X.

$$\begin{aligned} & \forall i \in \{1, 2, \ldots, n\}, \\ & f_i(U) < f_i(X) \wedge \\ & \exists j \in \{1, 2, \ldots, n\}, \\ & f_j(U) < f_j(X) \end{aligned} \tag{2}$$

If X^* is a Pareto optimal solution, there is no feasible solution X that can dominate X^*, which can be expressed by (2). The set of all Pareto optimal solutions is called Pareto optimal solution set. The curve or surface formed by the target vectors corresponding to all Pareto optimal solutions is called Pareto front.

$$\begin{aligned} & \nexists X \in R, \\ & F(X) < F\left(X^*\right) \end{aligned} \tag{3}$$

2.2. The Development of MMOSADE

2.2.1. Algorithm Improvement Strategy. Control parameters adaptive strategy is an important way to improve the performance of the differential evolution algorithm. MMOSADE adopts the control parameter index change strategy which is shown by (4)-(6) [10]. This control parameter adaptive strategy can ensure that the values of the mutation operator F and the cross operator CR are larger in the initial stage of calculation. The population can better cover the entire design space, by which the diversity of the population is improved and the global search is facilitated. With the advancement of the search process, the number of outstanding individuals in the population gradually increased. Appropriate reduction of mutation operator and crossover operator is helpful to reserve outstanding individuals, which is conducive to improving the probability of searching for the global optimal solutions.

$$F(t) = F_0 \cdot 2^{\lambda} \tag{4}$$

$$CR(t) = CR_0 \cdot 2^{\lambda} \tag{5}$$

$$\lambda = \exp\left(1 - \frac{T}{T + 1 - t}\right) \tag{6}$$

MMOSADE utilizes external archive method [11, 12] to achieve retention of outstanding individuals. When the MMOSADE starts, the external archive is empty. With the advancement of the evolutionary process, outstanding individuals enter the external archive. In terms of the diversity of external archives, MMOSADE introduces the crowding-distance calculation method of NSGA-II [13], and the calculation formula is shown by (7). However, this method also has certain defects. As is shown in Figure 1, the individuals A and B have the same crowding-distance by the crowding-distance calculation method. However, individual B is more crowded than A in fact.

$$d_i = \sum_{k=1}^{m} \frac{\left|f_k^{i+1} - f_k^{i-1}\right|}{\max f_k - \min f_k} \tag{7}$$

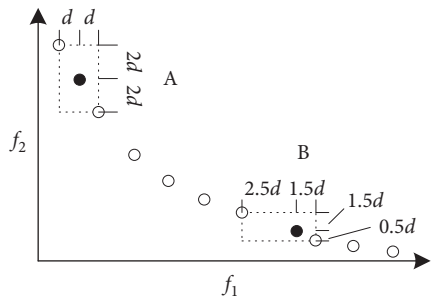

Figure 1: The method of space density estimating.

To further quantify individual density information, the concept of spatial density (SD) is proposed for the situation where two individuals have the same crowding-distance. The calculation method of the spatial density is shown by (8). It can be calculated that the spatial densities of individuals A and B are $10d^2$ and $11d^2$, respectively. The spatial density of B is larger than that of A. According to the principle of external archive diversity [13], the individual B is more crowded. Therefore, the individual A with lower density should be preferentially reserved.

$$\rho_i = \sum_{k=1}^{2} \left[\left(f_k^i - f_k^{i-1} \right)^2 + \left(f_k^{i+1} - f_k^i \right)^2 \right] \tag{8}$$

In terms of constraints processing, MMOSADE adopts the method of constrained dominance [14]. The main idea of this method is to deal with the objective function and the degree of violation of the constraint separately. The problem that the penalty factor is difficult to set in the penalty function method can be avoided by this method. For solution X and solution U, if any of the following conditions is met, then it can be considered that solution U constrain dominant solution X.

(1) Solution U is a feasible solution, and solution X is an infeasible solution.

(2) Both solution X and solution U are feasible solutions, and solution U dominates solution X.

(3) Both solution X and solution U are infeasible solutions, and the degree of U violation of the constraint is less than the solution X.

2.2.2. Algorithm Flow. The MMOSADE algorithm flow is shown in Figure 2.

2.3. MMOSADE Performance Test. The multiobjective optimization algorithm has two objectives [13]: (1) the obtained Pareto optimal solution set approximates the real Pareto optimal solution set and (2) maintains the diversity of the obtained solution set. Therefore, the performance of the multiobjective optimization algorithm is evaluated from two aspects: the convergence metric and the diversity metric [13].

(1) *Convergence Metric.* The convergence of the algorithm is evaluated by calculating the Generation Distance (*GD*). That is the degree of closeness between the calculated Pareto front and the true Pareto front. The calculation formula is as shown in (9).

$$GD = \frac{\sqrt{\sum_{j=1}^{n} d_j}}{n} \tag{9}$$

where n is the number of individuals in the obtained Pareto solution set. d_j is the minimum Euclidean distance of the i-th individual in the obtained Pareto solution set to the individual in the real Pareto solution set. The smaller *GD*, the better convergence of the algorithm.

(2) Diversity Metric. The diversity metric is evaluated by calculating the Spread (Δ), and the calculation formula is as shown by (10).

$$\Delta = \frac{d_f + d_l + \sum_{i=1}^{N-1} \left| d_j - \overline{d} \right|}{d_f + d_l + (n-1)\,\overline{d}} \tag{10}$$

where d_j is the Euclidean distance between two adjacent individuals in the obtained Pareto solution set. $\overline{d}$ is the mean of all d_j. d_l and d_f are the Euclidean distance between the extreme solutions and boundary solutions of obtained Pareto optimal solution set. The smaller the Δ, the better the distribution and diversity of the obtained Pareto optimal solution set.

In this paper, the performance of the algorithm is tested by the most widely used ZDT test function set [15]. The test results are compared with the three classical evolutionary algorithms of NSGA-II, SPEA2, and MOPSO. The population size of each algorithm is 100 and the maximum evolution algebra is 250. Tables 1 and 2, respectively, give the comparison results of the convergence index and diversity index of each algorithm running 30 times independently [14].

As is shown in Table 1, MMOSADE has a smaller *GD* than other algorithms when solving different classes of problems. This result indicates that the Pareto front obtained by the MMOSADE is more approximate the real Pareto front than other algorithms. It can be considered that MMOSADE has a better convergence metric than NSGA-II, SPEA 2, and MOPSO. In other words, MMOSADE can get the same precision Pareto front in a shorter time. Table 2 shows that MMOSADE has a better performance on solving the ZDT1 and ZDT6. Compared with NSGA-II, MMOSADE has a smaller Δ. These results verify that the proposed spatial density calculating method is effective and the diversity metric of MMOSADE is promoted notably. In summary, MMOSADE can be considered to have excellent solution performance. Therefore, MMOSADE can be utilized in the nuclear power system multiobjective optimization.

3. Nuclear Power System Multiobjective Optimization Design Platform

In this section, based on the MMOSADE algorithm, a multiobjective design platform for nuclear power system is developed and applied.

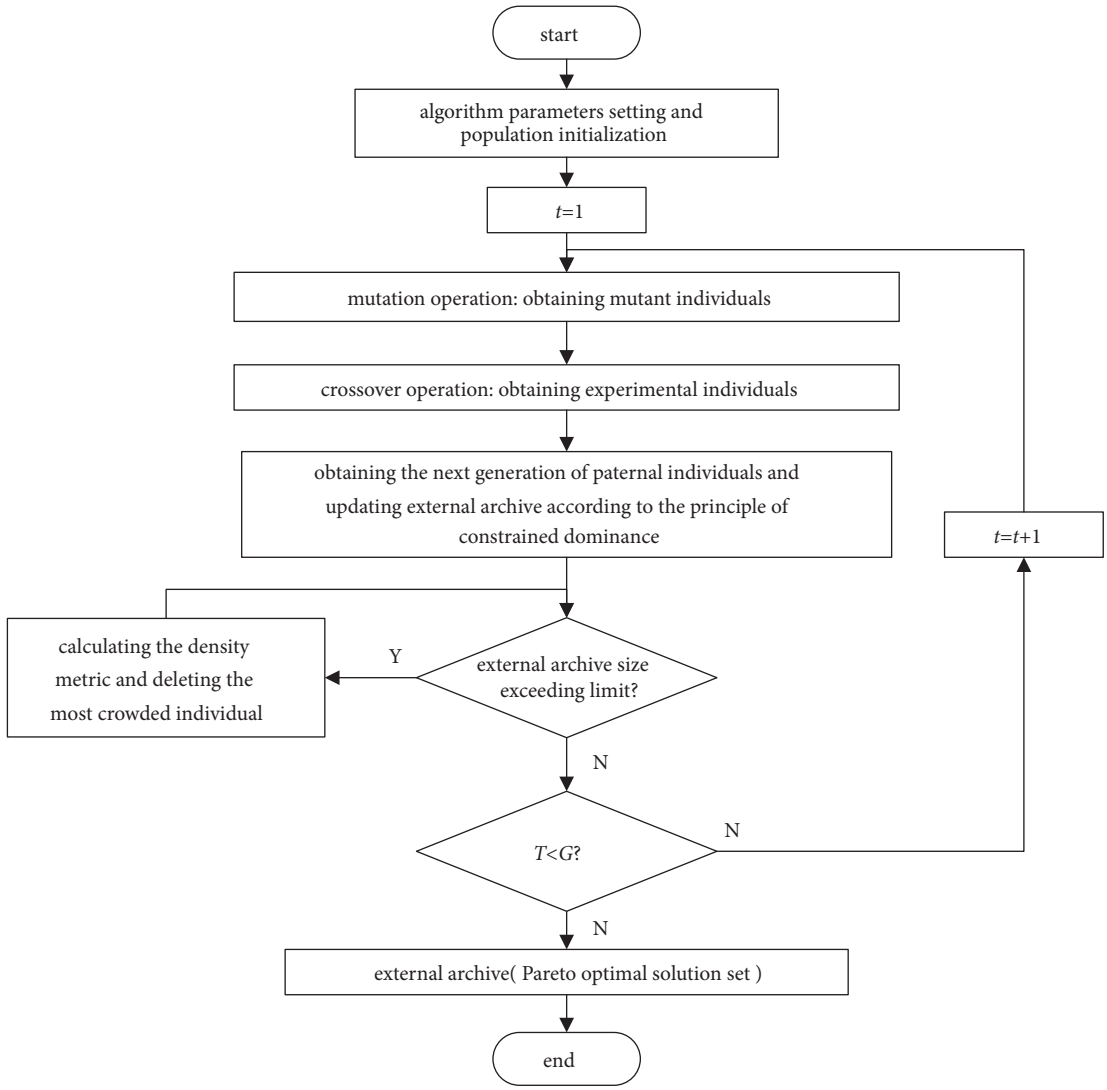

Figure 2: Flowchart of MMOSADE.

Table 1: Test results of convergence.

Test functions	NSGA-II Mean(Variance)	SPEA2 Mean(Variance)	MOPSO Mean(Variance)	MMOSADE Mean(Variance)
ZDT1	2.196e-4(6.6e-5)	1.575e-3(2.1e-2)	1.692e-2(1.1e-2)	*1.605e-4*(4.7e-5)
ZDT2	1.687e-4(4.6e-5)	4.995e-3(5.4e-3)	5.298e-2 (4.1e-2)	*1.268e-4* (3.0e-5)
ZDT3	3.532e-4 (1.3e-5)	1.701e-3 (4.2e-3)	4.869e-2 (9.0e-3)	*3.161e-4* (6.2e-5)
ZDT4	5.185e-4 (1.4e-4)	1.128e-1 (6.5e-3)	2.097e-1 (2.5e-1)	*3.516e-4* (8.3e-5)
ZDT6	7.943e-3 (1.1e-3)	1.915e-3 (1.6e-4)	1.992e-2 (5.3e-2)	*1.145e-4* (1.1e-5)

Table 2: Test results of variety.

Test functions	NSGA-II Mean(Variance)	SPEA2 Mean(Variance)	MOPSO Mean(Variance)	MMOSADE Mean(Variance)
ZDT1	5.007e-1 (3.0e-2)	2.676e-1 (1.8e-1)	2.949e-1 (2.7e-2)	*2.026e-1* (1.7e-2)
ZDT2	4.831e-1 (2.3e-2)	4.322e-1 (3.2e-1)	*2.851e-1* (1.6e-2)	3.133e-1 (1.1e-1)
ZDT3	5.881e-1 (4.8e-2)	*4.754e-1* (6.0e-2)	6.150e-1 (4.1e-3)	5.294e-1 (7.1e-2)
ZDT4	3.373e-1 (2.3e-2)	6.678e-1 (6.8e-1)	*3.145e-1* (5.2e-2)	4.220e-1 (9.9e-2)
ZDT6	4.946e-1 (4.4e-2)	2.363e-1 (2.8e-1)	1.156e-0 (1.3e-1)	*2.190e-1* (2.6e-2)

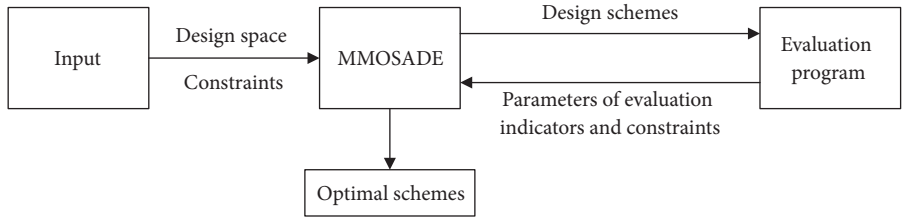

Figure 3: Diagram of nuclear power system multiobjective optimization design platform.

3.1. The Development of Nuclear Power System Multiobjective Optimization Design Platform. The optimization design platform for nuclear power system mainly includes three modules: (1) optimization object evaluation program module; (2) optimization algorithm module; (3) input module. The diagram of optimization design platform is shown in Figure 3.

The input module includes design space and constraints which are the basis of optimization calculation of the algorithm. According to the design space, MMOSADE produces the design schemes as the input parameters for the evaluation program. Then the parameters of evaluation indicators and constraints are calculated by the evaluation program. Combined with constraints, MMOSADE generates new design schemes based on the evaluation indicators. Finally, the optimal design schemes are obtained by several iterations.

3.2. The Application of Nuclear Power System Multiobjective Optimization Design Platform. The optimization design platform is utilized to optimize the PRHR-HX. In order to verify the reliability of the optimization design platform, the volume and the pressure loss of PRHR-HX are selected as the optimal targets. There is a certain mutual restriction between the above two indicators. What is more, the volume and the pressure loss are closely related to the economic and safety of nuclear power plants. The optimization variables are as follows: (1) the length of C-tube horizontal section L_h, (2) the length of C-tube vertical section L_v, and (3) C-tube outer diameter d_o.

3.2.1. PRHR-HX Calculation Model. The calculation model of PRHR-HX refers to the research of Ge et al.[16]. The structural diagram of the PRHR-HX is shown in Figure 4. The main structure includes a hemispherical inlet and outlet water chamber, a C-type heat transfer tube bundle, and a corresponding support structure [17]. The optimization is for the preliminary design of PRHR-HX in this paper, which is the steady-state design. Therefore, the following assumptions can be made [18]:

(1) All C-type heat transfer tubes of PRHR-HX have the same heat transfer performance.

(2) Ignore the thermal resistance of the dirt.

(3) The water temperature in the IRWST remains constant.

(4) The thermal conductivity of the tube wall is constant.

(5) Ignore the heat loss of components such as tube sheets.

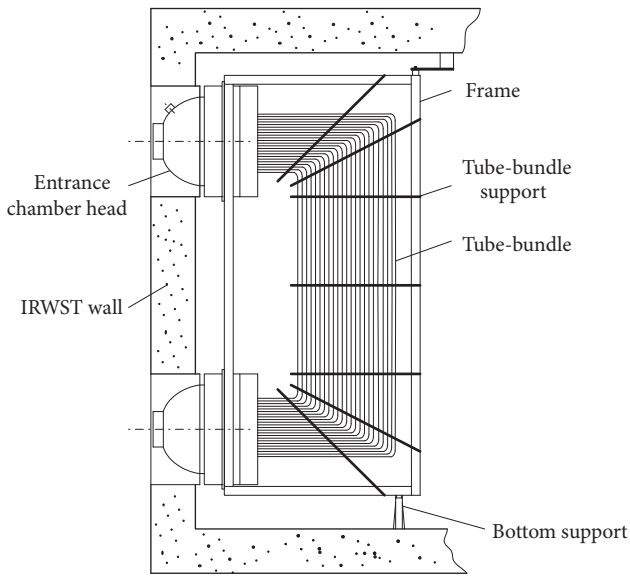

Figure 4: PRHR-HX structure diagram.

The mathematical model of PRHR-HX includes thermal calculation model and hydraulic calculation model.

(1) Thermal Calculation Model. The purpose of the thermal calculation is to obtain the heat transfer area of the PRHR-HX and the precise temperature distribution of the flow in the C-tube. The heat transfer process of PRHR-HX includes convective heat transfer on the tube side, heat conduction of the heat transfer tube, and natural convection and boiling heat transfer on the shell side.

The total heat transfer resistance of PRHR-HX can be expressed by (11).

$$R_{overall} = \frac{1}{\alpha_i} \cdot \frac{d_o}{d_i} + R_w + \frac{1}{\alpha_o} \tag{11}$$

According to the design requirements of the PRHR-HX, the Re_f of the fluid in the C-tube is larger than 6000 [19]. Therefore the flow in the C-tube is sufficient turbulent flow. The convection heat transfer equation in the tube can be calculated by the Dittus-Boelter formula (see (12)) [20].

$$Nu_f = \frac{\alpha_i d_i}{\lambda_f} = 0.023 Re_f^{0.8} Pr_f^{0.3} \tag{12}$$

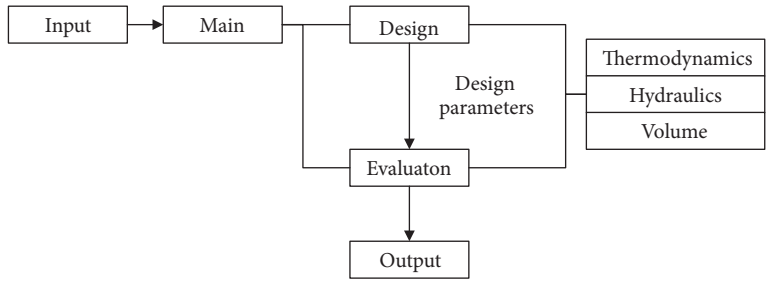

Figure 5: PRHR-HX evaluation procedure flow.

The thermal resistance of C-tube tube wall can be calculated by the following formula (see (13)).

$$R_w = \frac{d_o}{2\lambda_w} \ln\left(\frac{d_o}{d_i}\right) \tag{13}$$

If the C-tube outer wall surface temperature T_w is lower than the shell side saturation temperature T_{sat}, heat transfer mode is natural convection heat transfer in large space. The McAdams relations [21] are utilized.

The formula for calculating natural convection outside vertical tube is shown by (14) [21].

$$Nu_f = 0.13\left(Gr_f \cdot Pr_f\right)^{1/3} \tag{14}$$

The formula for calculating natural convection outside horizontal tube is shown by (15) [21].

$$Nu_f = 0.53\left(Gr_f \cdot Pr_f\right)^{1/4} \tag{15}$$

If the C-tube outer wall surface temperature T_w is larger than the shell side saturation temperature T_{sat} and the shell side fluid temperature T_f is lower than T_{sat}, the heat transfer mode outside the tube is nucleate boiling. Heat transfer coefficient is calculated by the Rohsenow relation [22] which is shown by (16).

$$h = h_b \frac{T_w - T_{sat}}{T_w - T_f} + h_n \tag{16}$$

h_b can be calculated according to (17).

$$h_b = \frac{c_{pl}^3 \left(T_w - T_{sat}\right)^2 \mu_l}{C_{sf}^3 Pr_l^3 h_{fg}^2} \sqrt{\frac{\sigma}{g\left(\rho_l - \rho_v\right)}} \tag{17}$$

(2) Hydraulic Calculation. The main purpose of hydraulic calculation is to obtain the pressure loss of PRHR-HX. The pressure loss can be calculated by (18) [23].

$$\Delta p = \left(\Delta p_f + \Delta p_r\right) F_t + \Delta p_s N_s \tag{18}$$

The friction pressure loss Δp_f can be calculated by (19).

$$\Delta p_f = f \frac{L}{d_i} \left(\frac{\rho u^2}{2}\right) \tag{19}$$

The flow pressure loss of the tube elbow Δp_r can be calculated by (20).

$$\Delta p_r = 3\left(\frac{\rho u^2}{2}\right) \tag{20}$$

The flow pressure loss of the inlet and outlet of water chamber Δp_s can be calculated by (21).

$$\Delta p_s = 1.5\left(\frac{\rho u^2}{2}\right) \tag{21}$$

Because the Re_f of the fluid in the C-tube is larger than 6000, friction coefficient f can be calculated according to the Haaland relation [24] which is shown by (22).

$$\frac{1}{\sqrt{f}} = -1.8 \lg\left(\left(\frac{3.7}{\varepsilon/D}\right)^{1.11} + \frac{6.9}{Re}\right) \tag{22}$$

3.2.2. Development and Verification of PRHR-HX Evaluation Program. Based on the PRHR-HX mathematical model, an evaluation program for system optimization is developed. The evaluation program mainly includes two modules (as is shown by Figure 5): (1) the design calculation module and (2) the evaluation calculation module. The main function of the design calculation module is to obtain the relevant design parameters that meet the design requirements by the input conditions and provide input for the evaluation calculation module. The main function of the evaluation calculation module is to obtain the value of evaluation indicators and constraints of PRHR-HX by the input conditions.

Input parameters are as follows: (1) PRHR-HX rated power P_e, (2) the length of C-tube horizontal section L_h, (3) the length of C-tube vertical section L_v, and (4) C-tube outer diameter d_o. The design parameters and evaluation indicators calculated by the evaluation program are taken as outputs. The calculation results are compared with the AP1000 prototype design parameters which are shown in Table 3. The results show that the thermal calculation results are accurate, and the calculation error of heat transfer area is only 0.33%. The hydraulic calculation error is relatively large, and the total pressure loss error is 2.64%. But it can still reflect the hydraulic characteristics of PRHR-HX. Therefore, it can be considered that the evaluation program is reliable and can be used to optimal design research.

Table 3: The comparison original design and calculating results.

Parameters	Prototype value	Calculated value	Relative error
The heat transfer area [m^2]	489	487.41	0.33%
The number of C-tube	689	687	0.29%
The inlet pressure loss [Pa]	750	730.12	2.65%
The C-tube pressure loss [Pa]	3700	3834.93	3.54%
The outlet pressure loss [Pa]	40	43.35	8.25%
The total pressure loss [Pa]	4490	4608.30	2.64%

Table 4: The parameters of optimal designs.

Parameters	Prototype scheme	Optimal scheme	Relative error
Volume [m^3]	6.42	6.35	1.02%
Pressure loss [kPa]	4.61	4.58	0.55%
L_h [m]	3.24	3.08	4.94%
L_v [m]	5.36	5.27	1.68%
d_o [m]	19.10	18.90	1.05%

3.2.3. Optimization Design of PRHR-HX. The two parameters of volume and pressure loss of PRHR-HX are selected as the evaluation index. The optimization variables include L_h, L_v, and d_o.

The constraints are as follows. (1) PRHR-HX is arranged in the in-containment refuelling water storage tank (IRWST), so its height should be less than the height of the IRWST. (2) To ensure the structural strength of the PRHR-HX, H_{HX}/D_e and H_{HX}/L_{HX} should be limited to a certain range. The specific boundaries of the constraints are as follows: (1) $H_{HX} \leq 6.15$m; (2) $4.8 \leq H_{HX}/D_e \leq 5.1$; (3) $1.6 \leq H_{HX}/L_{HX} \leq 1.8$; (4) $3\text{m} \leq L_h \leq 3.5\text{m}$; (5) $5\text{m} \leq L_v \leq 6\text{m}$; (6) $15\text{mm} \leq d_o \leq 25\text{mm}$.

The optimization results are shown by Figure 6. This figure shows that the distribution of the evaluation indicators of the optimal schemes (Pareto front). Combined with the actual engineering requirements and constraints, the engineer can select the appropriate scheme from the optimal schemes set according this figure.

3.3. Analysis of Optimization Results. If taking the smaller volume and pressure loss as the preferred standard, the better design scheme is as shown in the optimization scheme in Table 4. The volume of PRHR-HX is reduced by 1.02%. The pressure loss is reduced by 0.55%. It can be seen that the evaluation indicators of prototype scheme are similar to the optimal scheme. In this paper, some engineering constraints are not taken into account, such as the tolerance of equipment in manufacturing, processing and installation. That is, the optimal schemes obtained in this paper are idealized. For the actual design of PRHR-HX, the Pareto front should be above the obtained Pareto front. Therefore, considering the error of PRHR-HX evaluation program, it can be found that the prototype scheme is enveloped by the set of optimization schemes.

The AP1000 is recognized as a technologically advanced and mature nuclear power plant. It can be assumed that the design of PRHR-HX is fully optimized. The calculation results confirm this hypothesis. In the field of engineering design, the design method of PRHR-HX parameters is not disclosed. The prototype design scheme is enveloped by the optimal design schemes. This phenomenon reveals that the PRHR-HX prototype design is a Pareto optimal solution that meets the engineering requirements. This conclusion provides a new idea for the design of PRHR-HX. Additionally, the calculation results confirm that the multiobjective optimization design platform for nuclear power system is reliable and effective.

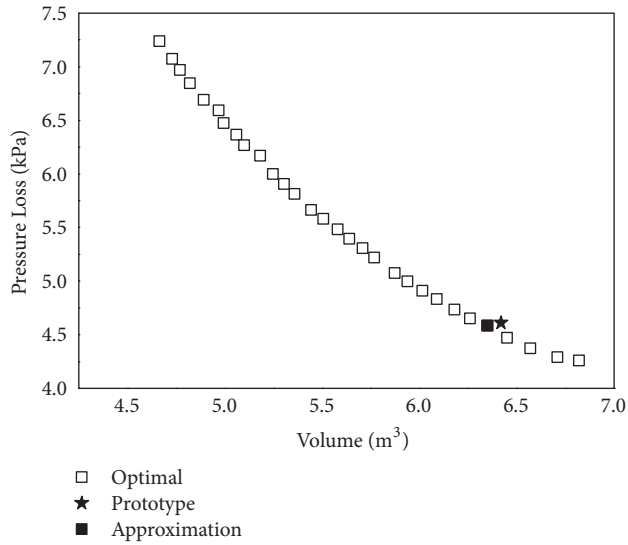

Figure 6: The distribution of original design and optimal designs.

4. Conclusion

In this paper, the MMOSADE algorithm is developed and its performance is tested. The nuclear power system optimization design platform is proposed based on the MMOSADE. The application research of the optimization design platform is carried out on AP1000 PRHR-HX. The conclusions are as follows.

(1) The proposed MMOSADE algorithm has better convergence than classical evolutionary algorithms and excellent diversity, and it can be used to solve such highly complex optimization problems such as nuclear power system optimization design.

(2) The multiobjective optimization design platform for nuclear power system can quickly and accurately obtain the set of PRHR-HX optimal design schemes, and the prototype design scheme is enveloped in the optimal schemes. On the one hand, it provides a new method for the design of PRHR-HX of different types reactor. On the other hand, the method can effectively solve the dual-objective optimization problem of nuclear power system.

(3) The nuclear power system optimization design platform can be utilized to optimize the design of different objects. It can avoid a lot of repetitive work in the research and development process; thus the development cycle can be shortened and the design efficiency can be improved to a certain extent.

Nomenclature

Abbreviations

MOP: Multiobjective optimization problem
DE: Differential evolution algorithm
MMOSADE: Modified multiobjective differential evolution algorithm
PRHR-HX: Passive residual heat removal heat exchanger
GD: Generation distance
IRWST: In-containment refuelling water storage tank
H_{HX}: PRHR-HX height
L_{HX}: PRHR-HX length
D_e: The tube bundle equivalent diameter
c_{pl}: Constant pressure specific heat capacity of the saturated liquid [J/(kg·°C)]
h_{fg}: Latent heat of vaporization [J/kg]
Pr_l: Prandtl number of the saturated liquid
μ_l: Dynamic viscosity of saturated liquid [Pa·s].

General Symbols for PRHR-HX

O_{verall}: Total heat transfer resistance of C-tube [$(m^2 \cdot °C)/W$]
α_i: Convective heat transfer coefficient in tube [$W/(m^2 \cdot °C)$]
α_o: Convective boiling heat transfer coefficient outside tube [$W/(m^2 \cdot °C)$]
d_o: C-tube outer diameter [m]
d_i: C-tube inner diameter [m]
R_w: Thermal resistance of C-tube tube wall [$(m^2 \cdot °C)/W$]
λ_f: Fluid thermal conductivity [W/(m·°C)]
λ_w: C-tube wall thermal conductivity [$(m^2 \cdot °C)/W$]
T_w: Outer wall surface temperature of C-tube [°C]
T_{sat}: Shell side saturation temperature
Re_f: Fluid Reynolds number
Gr_f: Fluid Grashof number
Pr_f: Fluid Prandtl number
h_n: Heat transfer coefficient when no nucleate boiling occurs [$W/(m^2 \cdot °C)$]
h_b: Heat transfer coefficient when nucleate boiling alone exists [$W/(m^2 \cdot °C)$]
L_h: The length of C-tube horizontal section [m]
L_v: The length of C-tube vertical section [m]
q: λ_l
q: Heat flux density [W/m^2]
ρ_l: Density of saturated liquid [kg/m^3]
ρ_v: Density of saturated steam [kg/m^3]
σ: Surface tension [N/m]
Δp_f: Friction pressure loss of C-tube [Pa]
Δp_r: Flow pressure loss of the tube elbow [Pa]
Δp_s: Flow pressure loss of the inlet and outlet of water chamber [Pa]
F_t: Structural correction factor
N_s: Number of water chambers
f: Coefficient of friction
L: Length of the runner [m]
ρ: Fluid density [kg/m^3]
u: Fluid velocity [m/s]
Δz: Potential difference between the inlet and outlet [m]
G: Mass flow density [$kg/(m^2 \cdot s)$]
ν_{out}: Specific volume of the inlet fluid [m^3/kg]
ν_{in}: Specific volume of the outlet fluid [m^3/kg].

Data Availability

The algorithm test results and optimal schemes of PRHR-HX used to support the findings of this study are available from the corresponding author upon request.

Conflicts of Interest

The authors declare that there are no conflicts of interest regarding the publication of this paper.

Authors' Contributions

Yunjia Yang is responsible for major research work and thesis writing, Shinian Peng is Yang's graduate tutor and is responsible for guiding research ideas, Li Zhu is Yang's graduate tutor and is responsible for guiding research ideas, Dan Zhang provides a lot of information on algorithm research and supports many suggestions for the revision of the paper, Zhifang Qiu provides information about AP1000, Hongsheng Yuan provides a lot of help in algorithm development, and puts forward many suggestions for the revision of the paper, and Lin Xian provides many suggestions for the revision of the manuscript and helps answer questions rasied by reviewers.

Acknowledgments

The authors would like to acknowledge the support of Nuclear Power Institute of China.

References

[1] C. Liu, C. Yan, and J. Wang, "Multi-objective optimization design on nuclear power primary circuit system," *Atomic Energy Science and Technology*, vol. 46, no. 12, pp. 1467–1472, 2012.

[2] L. Chen, H. Shi, and Q. Zeng, "The preliminary multi-objective optimization method of steam generators for marine nuclear propulsion plant," *Ship Engineering*, vol. 1, pp. 22–25, 1992.

[3] D. Liu and J. Yu, "Research on program for optimization design of nuclear power plant general parameters," in *Proceedings of the National Conference on Reactor Thermal Fluids*, Atomic Energy Press, Beijing, China, 1999.

[4] L. Chen, C. Yan, and J. Wang, "Multi-objective optimal design of vertical natural circulation steam generator," *Progress in Nuclear Energy*, vol. 68, pp. 79–88, 2013.

[5] L. Chen, C. Yan, and J. Wang, "Multi-objective optimal design for the coolant system of a pressurized power reactor and its validation by the RELAP5/MOD3.2 code," *Progress in Nuclear Energy*, vol. 71, pp. 216–224, 2014.

[6] L. Chen, C. Yan, Y. Liao, F. Song, and Z. Jia, "A hybrid non-dominated sorting genetic algorithm and its application on multi-objective optimal design of nuclear power plant," *Annals of Nuclear Energy*, vol. 100, pp. 150–159, 2017.

[7] D. Goldberg, *Genetic Algorithm in Search, Optimization and Machine Learning*, Addison-Wesley Publishing, Reading, Mass, USA, 1989.

[8] R. Storn and K. Price, "Differential evolution—a simple and efficient heuristic for global optimization over continuous spaces," *Journal of Global Optimization*, vol. 11, no. 4, pp. 341–359, 1997.

[9] Z. Bao and J. Yu, *Intelligent Optimization Algorithm and Its MATLAB Application*, Publishing House of Electronics Industry, Beijing, China, 2016.

[10] D. K. Tasoulis, N. G. Pavlidis, V. P. Plagianakos, and M. N. Vrahatis, "Parallel differential evolution," in *Proceedings of the 2004 Congress on Evolutionary Computation, CEC2004*, vol. 2, pp. 2023–2029, June 2004.

[11] E. Zitzler and L. Thiele, "Multiobjective evolutionary algorithms: A comparative case study and the strength Pareto approach," *IEEE Transactions on Evolutionary Computation*, vol. 3, no. 4, pp. 257–271, 1999.

[12] E. Zitzler, M. Laumanns, and L. Thiele, "SPEA2: Improving the strength Pareto evolutionary algorithm," Computer Engieering and Networks Lab (TIK), ETH Zurich, Switzerland, 2001.

[13] K. Deb, A. Pratap, S. Agarwal, and T. Meyarivan, "A fast and elitist multiobjective genetic algorithm: NSGA-II," *IEEE Transactions on Evolutionary Computation*, vol. 6, no. 2, pp. 182–197, 2002.

[14] L. Wu, *Research on Multi-Objective Dynamic Differential Evolution and Its Applications*, Hunan University, Hunan, China, 2011.

[15] E. Zitzler, K. Deb, and L. Thiele, "Comparison of multiobjective evolutionary algorithms: empirical results," *Evolutionary Computation*, vol. 8, no. 2, pp. 173–195, 2000.

[16] J. Ge, W. Tian, S. Qiu, and G. H. Su, "CFD investigation on thermal hydraulics of the passive residual heat removal heat exchanger (PRHR HX)," *Nuclear Engineering and Design*, vol. 327, pp. 139–149, 2018.

[17] H. Sun, P. Cheng, and H. Miao, *Third Generation Nuclear Power Technology AP1000*, China Power Press, Beijing, China, 2010.

[18] J. Dong and J. Wu, "Heat transfer analysis of the passive residual heat removal heat exchanger (PRHR HX)," *Applied Energy Technology*, vol. 4, pp. 19–22, 2014.

[19] T. Yonomoto, Y. Kukita, and R. R. Schultz, "Heat transfer analysis of the passive residual heat removal system in ROSA/AP600 experiments," *Nuclear Technology*, vol. 124, no. 1, pp. 18–30, 1998.

[20] S. Yang and W. Tao, *Heat Transfer*, Higher Education Press, Beijing, China, 1998.

[21] W. H. McAdams, *Heat Transmission*, McGraw-Hill, New York, NY, USA, 1954.

[22] L. Hao, G. Hu, and C. Guo, *Boiling Heat Transfer and Gas-Liquid Two-Phase Flow*, Harbin Engineering University Press, Harbin, China, 2016.

[23] S. Qian, *Heat Exchanger Design Handbook*, Chemical Industry Press, Beijing, China, 2002.

[24] E. J. Finnemore and J. B. Franzini, *Fluid Mechanics with Engineering Applications*, China Machine Press, Beijing, China, 2015.